Prediction of harmonic distortion generated by electro-dynamic loudspeakers using cascade of Hammerstein models

Marc Rébillat, Romain Hennequin, Etienne Corteel, Brian F.G. Katz

Prediction of harmonic distortion generated by electro-dynamic loudspeakers using cascade of Hammerstein models

Marc Rébillat*
Romain Hennequin†
Étienne Corteel‡
Brian F.G. Katz§

Abstract

Audio rendering systems are always slightly nonlinear. Their non-linearities must be modeled and measured for quality evaluation and control purposes. Cascade of Hammerstein models describes a large class of non-linearities. To identify the elements of such a model, a method based on a phase property of exponential sine sweeps is proposed. A complete model of non-linearities is identified from a single measurement. Cascade of Hammerstein models corresponding to an electro-dynamic loudspeaker are identified this way. Harmonic distortion is afterward predicted using the identified models. Comparisons with classical measurements techniques show that harmonic distortion is accurately predicted by the identified models over the entire audio frequency range for any desired input amplitude.

1 Introduction

Even if great efforts have been done to reduce or control their nonlinear behavior, loudspeakers are still the least linear part of the audio chain. The study of their non-linearities is thus of great importance. In electrodynamic loudspeakers, a motor converts the electrical signal in motion and makes a cone vibrate. The piston-like movement of the cone generates the sound field. The motor induces non-linearities because of non-uniform magnetic field, Eddy currents and variations of the electrical inductance with displacements [1, 2]. Significant excursion induces nonlinear bending in the cone and a nonlinear behavior of the suspensions [3].

Traditional nonlinear measurement methods [4] give total harmonic distortion (THD), harmonic distortion of order n (HD_n) or inter-modulation products (IMP) generated by loudspeakers. These quantities are measured using pure tones at a given amplitude and frequency. They do not describe non-linearities themselves but only some of their effects for these arbitrary excitations. Moreover, experimental processes involved in those methods are very time-consuming if a wide range of frequencies and amplitudes is to be covered. There is thus a real need for rapid model based procedures to measure non-linearities.

In order to represent the nonlinear behavior of electro-dynamical loudspeakers, different physical models have already been built. Their formulation was either completely analytical [5, 6] or based on the finite element method [7]. Klippel [8] proposed to use a Volterra series expansion [9] and identified it from measurements. However, all these physical models remains complex and heavy to manipulate. In Refs. [10, 11], it is thus suggested to use simpler nonlinear models, cascade of Hammerstein models, to represent and identify different audio systems, including acoustical transducers. Cascade of Hammerstein models [12] are a subclass of Volterra models and represents exactly systems having diagonal Volterra Kernels. These models are composed of N branches in parallel, made of one static polynomial non-linearity followed by one linear filter (see Fig. 1).

Some methods exist to identify the structural elements of a cascade of Hammerstein models. Gallman [12] and Hawksford [11] proposed a method using Gaussian noise at different amplitudes as inputs. The estimation procedures are strongly based on the knowledge of the order of non-linearity of the polynomial expansion, which is unknown in practical cases. Farina [10] proposed another method using sine sweeps with frequency varying exponentially with time. Only an upper bound of the order of non-linearity of the

*LIMSI (CNRS), B.P. 133, 91403 Orsay ,France and LMS (CNRS, École Polytechnique), 91128 Palaiseau, France
†Institut TELECOM (TELECOM ParisTech, CNRS LTCI), 46 Rue Barrault, 75013 Paris France
‡sonic emotion, Eichweg 6, CH-8154 Oberglatt (Zurich), Switzerland
§LIMSI (CNRS), B.P. 133, 91403 Orsay ,France

model has to be assumed. However this method permits the separation of the contributions of the different orders of non-linearity and not the complete identification of the Kernels of the system. Recently, Novák *et al.* [13] have identified Kernels from the contributions of the different orders of non-linearity using a least mean square minimization procedure. Of the examples given in Ref. [13], this method does not seem to be very accurate. An extension of the method of Farina [10] is proposed here. It yields directly all the Kernels of a cascade of Hammerstein models from the contributions of the different orders of non-linearity obtained as in Ref. [10].

In this paper, cascade of Hammerstein models corresponding to an electro-dynamical loudspeaker are identified using the previously introduced method from a single measurement. With the identified models, total harmonic distortion (THD) and $n^{\text{th}}-$order harmonic distortion (HD_n) are predicted for any desired amplitude and frequency. The THD and HD_n at different frequencies and amplitudes are also evaluated by classical means. The agreement between THD and HD_n predicted by the identified cascade of Hammerstein models and measured classically is very good in the entire audio frequency range, for a wide range of amplitudes. This method is thus a very reliable manner to quickly characterize non-linearities generated by electro-dynamic loudspeakers.

2 Mathematical foundations of the method

Mathematical foundations of the method used for direct identification of the elements of a cascade of Hammerstein models are given in this section. This method is an extension of the procedure initially proposed by Farina [10].

2.1 Cascade of Hammerstein models

A cascade of Hammerstein models is a nonlinear model made of N parallel branches. Each branch is composed of one nonlinear static polynomial element followed by a linear one $h_n(t)$ [12], as shown in Fig. 1.

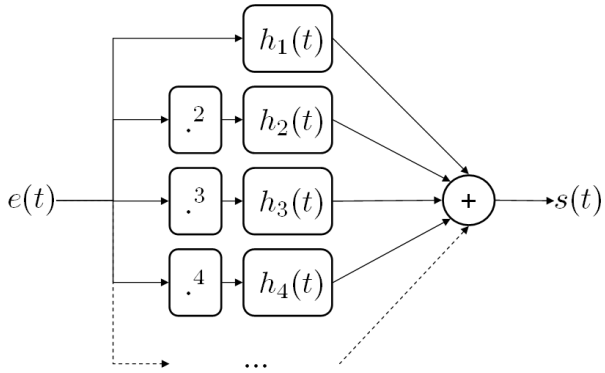

Figure 1: Block diagram representation of a cascade of Hammerstein models.

Mathematically, the relation between the input $e(t)$ and the output $s(t)$ of such a system is given by Eq. (1), where $*$ denotes the convolution.

$$s(t) = \sum_{n=1}^{N} h_n * e^n(t) \tag{1}$$

In this model, each impulse response $h_n(t)$ is convolved with the input signal elevated to its n^{th} power and the output $s(t)$ is the sum of these convolutions. The first impulse response $h_1(t)$ represents the linear response of the system. The other impulse responses $\{h_n(t)\}_{n\in\{2\dots N\}}$ model the non-linearities. All impulse responses are assumed to be zero-mean. The family $\{h_n(t)\}_{n\in\{1\dots N\}}$ will be referred to as the Kernels of the model. Any cascade of Hammerstein models is fully represented by its Kernels.

2.2 A cascade of Hammerstein models fed with sine sweeps

To experimentally cover the frequency range on which the system under study is to be identified, sines with time-varying frequencies are interesting signals:

$$\forall t \in \mathbb{R} \quad e(t) = \cos\left[\Phi(t)\right] \tag{2}$$

If $e(t)$ is the input of the cascade of Hammerstein models, the output of the nonlinear block of the i^{th} branch (see Fig. 1) is:

$$e^i(t) = \cos^i[\Phi(t)] \tag{3}$$

Using Chebyshev polynomials, $e^i(t)$ is rewritten in Eq. (4) as a linear function of $\{\cos[k\Phi(t)]\}_{k\in[1,i]}$. The coefficient of the matrix $\boldsymbol{C}$ of order 8 are given by Eq. (15)

$$\forall i \in \{1 \dots N\} \quad \cos^i[\Phi(t)] = \sum_{k=0}^{i} C(i,k)\cos[k\Phi(t)] \tag{4}$$

2.3 Exponential sine sweeps

When the instantaneous frequency of $e(t)$ is increasing exponentially from f_1 to f_2 ($f_1, f_2 > 0$) in a time T, such a signal is referred to as an "exponential sine sweep" [10, 14] and its instantaneous phase is given by :

$$\forall t \in \mathbb{R} \quad \Phi(t) = 2\pi \frac{f_1 T}{\ln \frac{f_2}{f_1}} (e^{\frac{t}{T}\ln\frac{f_2}{f_1}} - 1) - \pi/2 \tag{5}$$

The corresponding instantaneous frequency of $e(t)$ is :

$$\forall t \in \mathbb{R} \quad f(t) = \frac{\Phi'(t)}{2\pi} = f_1 e^{\frac{t}{T}\ln\frac{f_2}{f_1}} \tag{6}$$

Thus $f(0) = f_1$ and $f(T) = f_2$. The frequency range $[f_1, f_2]$ corresponds to the band of interest of the system under test.

2.4 Fundamental phase property

From Eq. (5), it can be shown that this type of signal exhibits the phase property given by Eq. (7).

$$\begin{aligned} &\forall k \in \mathbb{N}^*, \forall t \in \mathbb{R} \ : \\ &k\Phi(t) = \Phi(t + \frac{T\ln k}{\ln \frac{f_2}{f_1}}) - (k-1)(\frac{\pi}{2} + \frac{2\pi f_1 T}{\ln \frac{f_2}{f_1}}) \end{aligned} \tag{7}$$

By choosing $T_m = (2m\pi - \frac{\pi}{2})\frac{\ln f_2/f_1}{2\pi f_1}$ with $m \in \mathbb{N}^*$, the second term in Eq. (4) becomes a multiple of 2π and one obtains Eq. (8) which is another way to express the k^{th} term of the linearization given in Eq. (4).

$$\forall k \in \mathbb{N}^*, \quad \cos\left[k\Phi(t)\right] = \cos\left[\Phi(t + \Delta t_k)\right] \tag{8a}$$

$$\text{with} \quad \Delta t_k = \frac{T_m \ln k}{\ln f_2/f_1} \tag{8b}$$

For any T_m-long logarithmic sweep, multiplying the phase by a factor k results in the same signal, but in advance in the time domain by Δt_k. As can be seen from Eqs. (8a) and (8b), this time advance depends only on the sweep parameters T_m, f_1, f_2 and on k. In Refs. [10, 15], similar time advances were obtained using different arguments.

The fact that T_m must take only a discrete set of values to ensure the fundamental phase property (8a) has been first highlighted in Ref. [13] but is mathematically demonstrated here for the first time.

One should note that $e(t)$ has been designed for all t with its instantaneous frequency increasing from f_1 to f_2 between $t = 0$ and $t = T$. In practice, signals are defined only on $[0, T]$. Thus the phase property is not valid on the whole support of the function. The phase property becomes false when the instantaneous frequency of $\cos\left[k\Phi(t)\right]$ is outside the frequency range of interest (i.e. $[f_1, f_2]$).

2.5 Inverse convolution

Using the Eqs. (8a) and (1), one obtains:

$$\begin{aligned} s(t) &= \sum_{n=1}^{N} g_n * e(t + \Delta t_n) \\ \text{with} \quad g_n(t) &= \sum_{k=n}^{N} C(k,n) h_k(t) \end{aligned} \tag{9}$$

In order to separately identify each Kernel of the cascade of Hammerstein models, a signal $y(t)$ which looks like an inverse in the convolution sense of $e(t)$ is needed. Unfortunately, such an inverse does not necessarily exist mathematically. A band-limited inverse $y(t)$ can however easily be defined such that it satisfies:

$$y(t) * e(t) = \text{sinc}(2f_2 t) - \text{sinc}(2f_1 t) = d(t) \tag{10}$$

with $\text{sinc}(x) = \sin(\pi x)/\pi x$.

$d(t)$ can be seen as a band-limited Dirac Function, since its Fourier transform is $\mathbb{1}_{[-f_2,-f_1]\cap[f_1,f_2]}(f)$. Then, $Y(f)$, the Fourier transform of the inverse filter $y(t)$ can be built in the frequency domain using Eq. (11).

$$\begin{aligned} Y(f) &= \frac{1}{E(f)} \mathbb{1}_{[-f_2,-f_1]\cap[f_1,f_2]}(f) \\ &\simeq \frac{1}{E(f)} \frac{1}{1+\epsilon(f)} \end{aligned} \tag{11}$$

In practice, the filter $Y(f)$ should be build by replacing the discontinuous function $\mathbb{1}_{[-f_2,-f_1]\cap[f_1,f_2]}(f)$ by a function of the type $\dfrac{1}{1+\epsilon(f)}$. This function ensures a smoother transition between the two frequency domains and thus generates less unwanted side effects in the time domain.

$\epsilon(f)$ is a frequency dependent real parameter chosen as equal to 0 in the bandwidth and as having a large value outside of it, with a continuous transition between the two domains.

In so doing, $y(t)$ can be considered as an inverse of $e(t)$ in the sense of convolution in the frequency range $[f_1, f_2]$.

2.6 Kernels Identification in the temporal domain

After convolving the output of the cascade of Hammerstein models $s(t)$ given in Eq. (9) with $y(t)$, one obtains :

$$y * s(t) = \sum_{i=1}^{N} g_i(t + \Delta t_n) * d(t) \tag{12}$$

Since it is assumed that the system under study has no significant behavior outside $[f_1, f_2]$, $g_i(t + \Delta\, t_n) * d(t)$ reduces to $g_i(t + \Delta t_n)$, and then :

$$y * s(t) = \sum_{i=1}^{N} g_i(t + \Delta t_n) \tag{13}$$

In Fig. 2, $y * s(t)$ is represented. Because $\Delta t_n \propto \ln(n)$ and $f_2 > f_1$, the higher the order of linearity n is, the more in advance the corresponding $g_n(t)$ will be. Thus, if T_m is long enough, the different $g_n(t)$ will not overlap. It is then easy to separate them by windowing in the time domain. The separation of the contribution of the different orders of non-linearity by using exponential sweeps, which is mathematically demonstrated here, is already experimentally well known in the audio community [14, 16, 17].

After that step, using Eq. (14), the family $\{h_n(t)\}_{n\in[1,N]}$ of the Kernels of the cascade of Hammerstein models can be fully extracted.

$$\begin{pmatrix} h_1(t) \\ \vdots \\ h_N(t) \end{pmatrix} = \boldsymbol{A}_c^T \begin{pmatrix} g_1(t) \\ \vdots \\ g_N(t) \end{pmatrix} \tag{14}$$

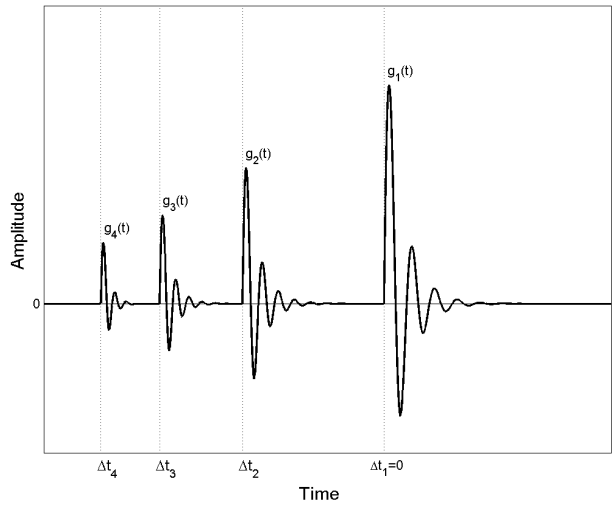

Figure 2: Separation of the different order of non-linearity after convolution with $y(t)$.

The matrix $\boldsymbol{A}$ of order 8, which is sufficient for practical use, is given in Eq. (15). $\boldsymbol{A}_c^T$ is the matrix $\boldsymbol{A}^T$ without the first column and the first row, and $(.)^T$ stands for matrix transposition. Then, as all the Kernels of the system are known, the system under study is completely identified.

$$\boldsymbol{A} = \boldsymbol{C}^{-1} = \begin{pmatrix} 1 & 0 & 0 & 0 & 0 & 0 & 0 & 0 \\ 0 & 1 & 0 & 0 & 0 & 0 & 0 & 0 \\ -1 & 0 & 2 & 0 & 0 & 0 & 0 & 0 \\ 0 & -3 & 0 & 4 & 0 & 0 & 0 & 0 \\ 1 & 0 & -8 & 0 & 8 & 0 & 0 & 0 \\ 0 & 5 & -20 & 0 & 0 & 16 & 0 & 0 \\ -1 & 0 & 18 & 0 & -48 & 0 & 32 & 0 \\ 0 & -7 & 0 & 56 & 0 & -112 & 0 & 64 \end{pmatrix} \tag{15}$$

3 Practical implementation

In this section, the practical discrete-time implementation of the method presented in section 2 is described.

3.1 Overview of the method

In Fig. 3, a global overview of the procedure is given. It can be decomposed in the following steps:

1. Design of the input sweep $e(t)$ using Eq. (5). The choice of f_1, f_2 and T is discussed in section 3.2.
2. Playing $e(t)$ and recording $s(t)$. The sampling frequency f_s must be chosen to avoid any aliasing effects caused by the digital to analog converter in the frequency range of interest $[f_1, f_2]$.
3. Generation of the inverse filter $y(t)$ according to Eq. (11). A convenient way to implement this filter is described in section 2.5.
4. Convolution of the output signal $s(t)$ with the inverse filter $y(t)$ as in Eq. (13). This can be done in the frequency domain with a sufficient number of points to avoid temporal aliasing.
5. Windowing in the temporal domain (cf. Fig. 2) to obtain the $\{g_k(t + \Delta t_k)\}_{k\in[1,N]}$. Rectangular windows of constant size $\tau = 1/2(\Delta t_N - \Delta t_{N-1})$ can be chosen to separate the different orders of non-linearity. N is the highest desired order in the cascade Hammerstein model.
6. Temporal shift of the different orders of non-linearity to recover $\{g_k(t)\}_{k\in[1,N]}$. A shift of a non-integer number of samples can be performed with a phase shift in the frequency domain.
7. Multiplication with $\boldsymbol{A}_c^T$ to access $\{h_k(t)\}_{k\in[1,N]}$, according to Eq. (14). The matrix $\boldsymbol{A}$ of order 9 is given in Eq. (15).

3.2 Choice of the parameters (f_1, f_2, T and N)

For satisfactory measurements, the sweep parameters f_1, f_2, T and N must be well chosen. These choices must be made considering the following aspects:

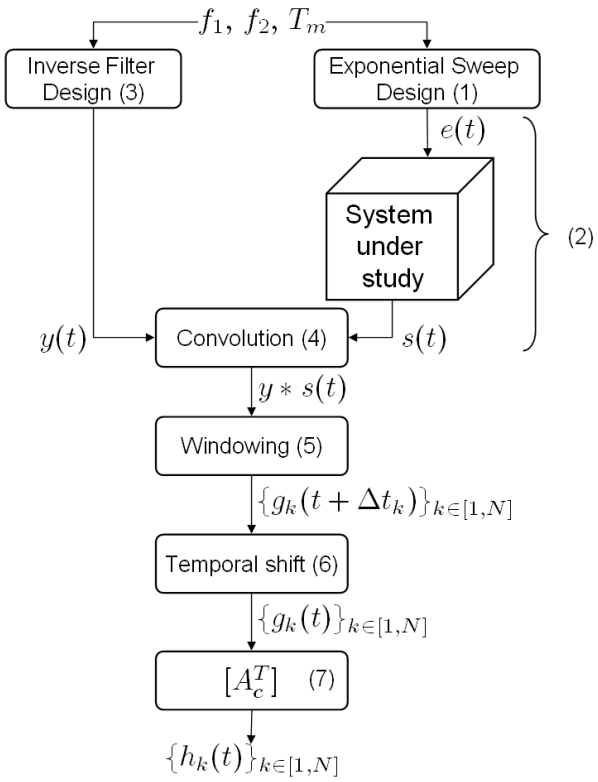

Figure 3: Overview of the method used to identify a Cascade of Hammerstein models.

- The frequencies f_1 and f_2 must be chosen such that the interesting behavior of the system under study is in the frequency range $[f_1, f_2]$.
- The influence of noise on the identification results should also be minimized [15]. By itself, the exponential sweep rejects correctly uncorrelated noise in quiet environment [18]. Moreover its energy repartition in frequency is often adapted to the ambient noise [17, 19]. The choice of this signal is thus interesting from this point of view. If an excellent signal to noise ratio (SNR) is needed, the longer T, the better the SNR after step 4 will be at a given amplitude of the input signal.
- The number of points to be convolved at step 4 is limited by the available computational power. Thus, as T increases, the computation time will increase. T must not be too high in order to avoid long calculation time.
- N should not be underestimated to guarantee good accuracy in identification. The optimal N is reached when it is impossible to extract the corresponding N^{th} impulse response from the background noise.
- The different pseudo-impulse responses $g_k(t)$ which appear in the temporal domain after the convolution with the inverse signal (step 4, see Fig. 2) must not overlap each other. The global decay time of the system τ_{global} is an upper bound of the decay times of each orders of non-linearity. Parameters f_1, f_2 and T such that $\Delta t_N - \Delta t_{N-1} > \tau_{\text{global}}$ will thus avoid overlapping of the different orders of non-linearity [19, 20]. Because $\Delta t_N = \dfrac{T_m \ln N}{\ln f_2/f_1}$, considering the chosen value for N, T must be chosen to be long enough and f_2/f_1 not so large in order to respect the previous condition.

4 Modeling electro-dynamic loudspeakers with cascade of Hammerstein models

In this section, an electrodynamic loudspeaker is identified as cascade of Hammerstein models using the method presented in section 2.

4.1 Experimental setup

Experiments have been conducted on a standard electrodynamic loudspeaker. All measurements have been made on axis at one meter from the motor with a microphone. Measurements have been done in a semi-anechoic room. In these conditions, a signal to noise ratio of $\simeq 50$ dB below 50 Hz and of $\simeq 70$ dB above has been reached for pressure amplitudes of $\simeq 110$ dB.

4.2 Measured cascade of Hammerstein models Kernels

The Kernels corresponding to the system have been measured using the previously described experimental setup. As the cascade of Hammerstein models is a nonlinear model, its Kernels should be independent of the amplitude of measurement. To assess this, measurements of the Kernels have been done using parameters given in Tab. 1 for 10 different amplitudes ranging from 95 to 115 dB in pressure.

Parameter	Value
f_1	20 Hz
f_2	20 kHz
f_s	192 kHz
T	15 s
N	5

Table 1: Parameters chosen to identify the simulated system.

Mean measured Kernels and their corresponding standard deviation are given in Fig. 4 for the electro-dynamical loudspeaker. The amplitude of the different Kernels of order $n \geq 2$ decreases with frequency, which is consistent with the physical analysis of [6]. The linear part, which is by definition independent of the amplitude, exhibits no variations among the different measurements. The non-linearities have thus been removed successfully from the linear part using the proposed method. The identified Kernels of order $n \geq 2$ depends slightly on the amplitude at which they have been measured. As a consequence, the assumption that electro-dynamic loudspeakers can be represented by cascade of Hammerstein models is a correct approximation in the chosen range of amplitudes.

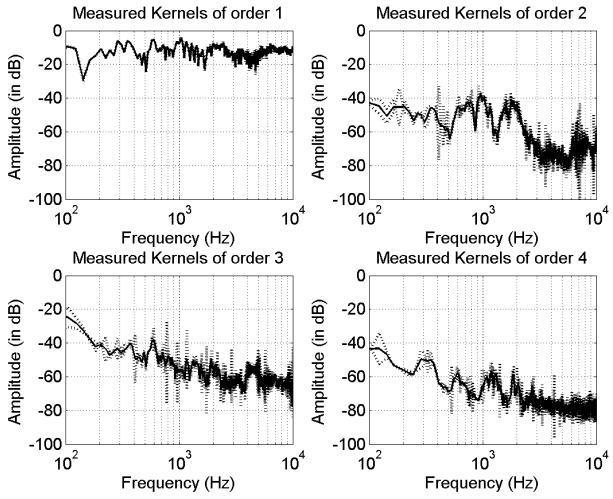

Figure 4: Mean measured Kernel of the cascade of Hammerstein models (solid line) and the corresponding standard deviations (dashed lines).

5 Prediction of the harmonic distortion generated by transducers

In this section, the previously identified cascade of Hammerstein models will be used to predict the harmonic distortion generated by the electro-dynamic loudspeaker.

5.1 Link between HD_n, THD and cascade of Hammerstein models

To characterize distortion generated by an acoustic transducer, the following approach is classically adopted. The input of the system is assumed to be sinusoidal, and non-linearities generate harmonic components at frequencies higher than the input fundamental frequency. The amplitudes of these harmonics compared to the amplitude of the fundamental are considered as representative of the non-linearity of the transducer. Total harmonic distortion (THD) and harmonic distortion of order n (HD_n) are common tools to quantify this [4]. The THD is the square root of the ratio of the power contained in the harmonics to the power contained in the fundamental. The HD_n is the same but for the n^{th} harmonic only.

For a sinusoidal input signal $x(t) = X\cos(2\pi ft)$ which enters a cascade of Hammerstein models identified at the amplitude X_0, the output signal $z(t)$ can be written as in Eq. (16) by using Eqs. (1) and (4).

$$\begin{aligned} z(t) &= \sum_{n=1}^{N} |\Gamma_n(X, nf)| \cos\left[2\pi nft + \angle(\Gamma_n(X, nf))\right] \\ \text{with} \quad \Gamma_n(X, f) &= \sum_{k=1}^{N} \left(\frac{X}{X_0}\right)^k C(k, n) H_k(f) \end{aligned} \tag{16}$$

THD and HD_n can thus be directly identified from Eq. (16) and expressed as:

$$\mathrm{HD}_n(X, f) = \left|\frac{\Gamma_n(X, nf)}{\Gamma_{\mathrm{Tot}}(X, f)}\right| \tag{17a}$$

$$\mathrm{THD}(X, f) = \sqrt{\sum_{n=2}^{N} \left[\frac{\Gamma_n(X, nf)}{\Gamma_{\mathrm{Tot}}(X, f)}\right]^2} \tag{17b}$$

$$\text{with} \quad \Gamma_{\mathrm{Tot}}(X, f) = \sqrt{\sum_{n=1}^{N} [\Gamma_n(X, nf)]^2} \tag{17c}$$

The knowledge of the Kernels in the frequency range $[f_1, f_2]$ allows for the direct computation of the THD and HD_n using Eqs. (17). This can be done for any value of input amplitude X and for any frequency f in $[f_1, f_2]$. In the present study, the prediction of the inter-modulation product (IMP) has not been included for the sake of brevity. Nevertheless, this model is fully able also to predict IMP, or to compute the output corresponding to any desired signal.

5.2 Prediction of HD_n and THD at a given amplitude

Using the different sets of Kernels measured in the previous section, the HD_n and THD have been predicted from Eqs. (17). To compare with, traditional measurements using pure tones have been done using the experimental protocol depicted in section 4.1. HD_n and THD have been measured this way for 50 frequencies between 50 Hz and 12 kHz and for 10 different amplitudes ranging from 95 to 115 dB in pressure. In Fig. 5 the predictions made using equations (17) with identified Kernels and the traditional measurements are shown. It can be seen that the agreement between measured and predicted data is very good over the entire frequency range.

5.3 Prediction of HD_n and THD for different amplitudes

To have an overview of the quality of the predictions depending on the amplitude at which Kernels have been measured (X_{m}) and on the amplitude at which prediction are made (X_{p}), a mean error has been introduced. This error is defined in Eq. 18. This error has been computed for the following frequency bands: $[45, 355]$ Hz (octave bands centered at 63 Hz, 125 Hz, and 250 Hz), $[355, 2800]$ Hz (octave bands centered at 500 Hz, 1 kHz and 2 kHz) and $[2800, 11200]$ Hz (octave bands centered at 4 kHz and 8 kHz). The error in dB in each of these frequency bands is shown in Fig. 6.

$$\begin{aligned} &\Delta_{[f_A, f_B]}(X_{\mathrm{m}}, X_{\mathrm{p}}) = ... \\ &20\log_{10} \underset{[f_A, f_B]}{\mathrm{mean}} \left|\mathrm{THD}^{\mathrm{m}}(X_{\mathrm{p}}, f) - \mathrm{THD}^{\mathrm{p}}(X_{\mathrm{m}}, X_{\mathrm{p}}, f)\right| \end{aligned} \tag{18}$$

In Fig. 6 (a), the error in the frequency band $[45, 355]$ Hz is shown. It can be seen that this error is low, around -11 dB. The minimum of -15 dB is reached when the THD is predicted for low values of X_{p}.

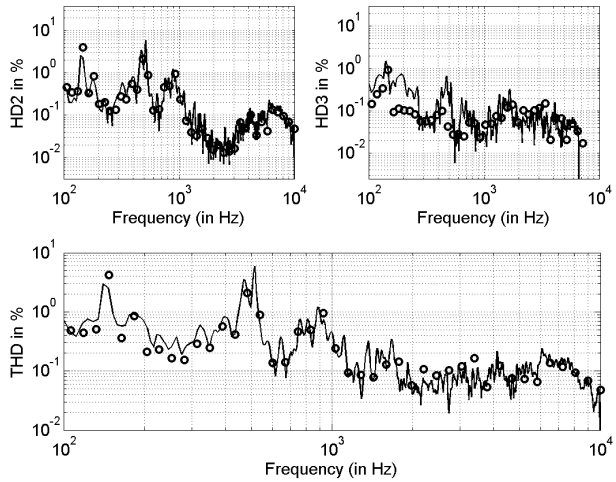

Figure 5: Comparisons between measurements (circles) and predictions (solid lines) at 106 dB for the HD_2, HD_3 and THD. Kernels identified at 107 dB have been used for predictions.

As the amplitude of prediction X_p increases, the error increases too in this frequency band, but with still a very good accuracy. In Figs. 6 (b) and (c), errors for frequency bands $[355, 2800]$ and $[2800, 11200]$ Hz are shown. Error values in these frequency bands are significantly lower than in the previous one. The minimums of these errors, which are -25 dB and -21 dB, can be seen around the diagonals. Predictions are then very precise in these frequency bands.

6 Conclusion

In this article a method for the identification of a class of nonlinear systems, referred to as cascade of Hammerstein models, has been mathematically described and applied on an electro-dynamic loudspeakers. This method permits the complete identification of the constitutive elements of the model from only one single measurement. This method is very fast compared to other methods [11, 12] where several repeated measurements are necessary. The mathematical formalism developed by the authors allows moreover an extension beyond the simple separation of the different orders of non-linearities initially proposed by Farina [10].

Harmonic distortion of order n (HD_n) and the total harmonic distortion (THD) are afterwards predicted using the identified Kernels. The originality of the present approach is that HD_n and THD are predicted at different amplitudes. This is an advance compared to the literature where HD_n and THD are usually predicted only for a given amplitude [5, 10, 19]. Results obtained when comparing this approach to the traditional one at different amplitudes for HD_n and THD are very satisfying.

This method is also interesting for transducer quality assessment. Indeed, the present approach gives a straightforward access to a compact and very fine representation of the linear and nonlinear characteristics of real transducers. As has been shown in this paper, total harmonic distortion and n^{th}-order harmonic distortion are precisely predicted by the identified models. However, they badly correlate with subjective experiments involving transducer's quality [21]. Nevertheless, as an input-independent model is available, simulations of the nonlinear responses of identified transducers for any desired input signal (noise, music, ...) can be easily performed. This can be very useful when searching pertinent cues to assess the decreases of quality caused by non-linearities in acoustical transducers.

In a future work, models of panel-based transducers (distributed mode loudspeakers [22] or multi-actuator panels [23]) will be identified with the present method. As their physical underlying principle is different it is not obvious that cascade of Hammerstein models represent them correctly. The influence of the order of non-linearity N and the sensitivity of the method to ambient noise will also be studied.

References

[1] W. Klippel. Tutorial: Loudspeaker nonlinearities - causes, parameters, symptoms. *Journal of the Audio Engineering Society*, 54(10):907–939, 2006.

[2] M. Colloms, J. Panzer, V. Gotcharov, and V. Taylor. Distortion mechanisms of distributed mode (DM) panel loudspeakers. *104th Convention of the Audio Engineering Society*, 1998.

[3] N. Quaegebeur and A. Chaigne. Nonlinear vibrations of loudspeaker-like structures. *Journal of Sound and Vibration*, 309(1-2):178–196, 2008.

[4] E. Czerwinski, A. Voishvillo, S. Alexandrov, and A. Terekhov. Multitone testing of sound system components some results and conclusions - part 2: Modeling and application. *Journal of the Audio Engineering Society*, 49(12):1181–1192, 2001.

[5] A. J. M. Kaizer. Modeling of the nonlinear response of an electrodynamic loudspeaker by a volterra series expansion. *Journal of the Audio Engineering Society*, 35(6):421–433, June 1987.

[6] W. Klippel. Modeling the nonlinearities in horn loudspeakers. *Journal of the Audio Engineering Society*, 44(6):470–480, June 1996.

[7] T. Tsuchiya, Y. Kagawa, M. Doi, and T. Tsuji. Finite element simulation of non-linear acoustic generation in a horn loudspeaker. *Journal of Sound and Vibration*, 266(5):993–1008, October 2003.

[8] W. Klippel. Nonlinear system identification for horn loudspeakers. *Journal of the Audio Engineering Society*, 44(10):811–820, October 1996.

[9] M. Hasler. *Phénomènes non linéaires, Chapitre 3 : Séries de Volterra*. EPFL Lausanne, 1999.

[10] A. Farina. Simultaneous measurement of impulse response and distortion with a swept-sine technique. *108th Convention of the Audio Engineering Society*, 2000.

[11] M. O. J. Hawksford. System measurement and identification using pseudorandom filtered noise and music sequences. *Journal of the Audio Engineering Society*, 53(4):275–296, April 2005.

[12] P. G. Gallman. Iterative method for identification of nonlinear-systems using a Uryson model. *IEEE Transactions on Automatic Control*, 20(6):771–775, 1975.

[13] A. Novák, L. Simon, P. Lotton, and Kadlec F. Modeling of nonlinear audio systems using swept-sine signals: application to audio effects. *12th International Conference on Audio Effects*, 2009.

[14] S. Norcross and J. Vanderkooy. A survey on the effects on nonlinearity on various types of transfert-function measurements. *99th Convention of the Audio Engineering Society*, 1995.

[15] M. Morise, T. Irino, H. Banno, and H. Kawahara. Warped-TSP: An acoustic measurement signal robust to background noise and harmonic distortion. *Electronics and Communications in Japan Part III-Fundamental Electronic Science*, 90(4):18–26, 2007.

[16] P. G. Craven and M. A. Gerzon. Practical adaptative room and loudspeaker equaliser for hi-fi use. *92th Convention of the Audio Engineering Society*, 1992.

[17] D. Griesinger. Beyond MLS - occupied hall measurerement with FFT techniques. *101th Convention of the Audio Engineering Society*, 1996.

[18] G. B. Stan, J. J. Embrechts, and D. Archambeau. Comparison of different impulse response measurement techniques. *Journal of the Audio Engineering Society*, 50(4):249–262, 2002.

[19] S. Muller and P. Massarani. Transfer-function measurement with sweeps. *Journal of the Audio Engineering Society*, 49(6):443–471, 2001.

[20] P. Majdak, P. Balazs, and B. Laback. Multiple exponential sweep method for fast measurement of head-related transfer functions. *Journal of the Audio Engineering Society*, 55(7-8):623–637, 2007.

[21] Alex Voishvillo. Assessment of nonlinearity in transducers and sound systems - from thd to perceptual models. *121th Convention of the Audio Engineering Society*, 2006.

[22] N. J. Harris and M. O. J. Hawksford. Introduction to distributed mode loudspeakers (DML) with first-order behavioural modelling. *IEEE Proceedings - Circuits, Devices and Systems*, 147(3):153–157, 2000.

[23] M. Kuster, D. De Vries, D. Beer, and S. Brix. Structural and acoustic analysis of multiactuator panels. *Journal of the Audio Engineering Society*, 54(11):1065–1076, 2006.

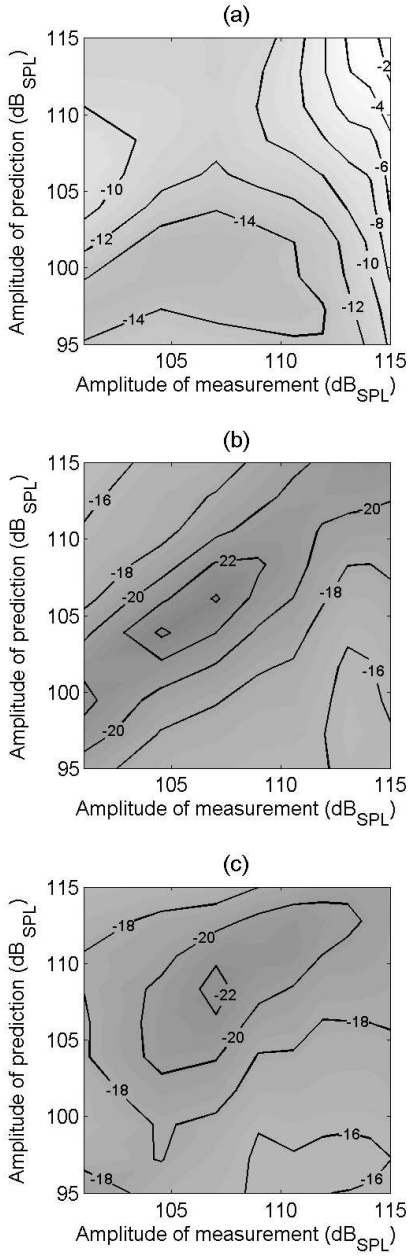

Figure 6: Mean error in the frequency band $[45, 355]$ (a), $[355, 2800]$ (b) and $[2800, 11200]$ Hz (c) for the electrodynamic loudspeaker. Amplitudes of measurement of the Kernels are given on the x-axis.